# Fully-Etched Grating Coupler with Low Back Reflection

Yun Wang[a], Wei Shi[b], Xu Wang[a], Jonas Flueckiger[a], Han Yun[a], Nicolas A. F. Jaeger[a], and Lukas Chrostowski[a]

[a] The University of British Columbia, 2329 West Mall, Vancouver, Canada;
[b] Université Laval, Québec City, Canada;

## ABSTRACT

A fully-etched grating coupler with improved back reflection and bandwidth is demonstrated in this paper. It can also be made in compact patterns with much smaller footprints than conventional, fully-etched grating couplers with long adiabatic tapers. Sub-wavelength gratings were employed to form the effective index areas between the major gratings. Our grating has a measured 3-dB bandwidth of 64.37 nm with a back reflection of -14 dB.

**Keywords:** silicon photonics, grating coupler, fully-etched

## 1. INTRODUCTION

Silicon photonics, implemented on silicon-on-insulator (SOI), is a very promising technology for photonics integrated circuits. Due to the large refractive index contrast between the silicon core and the cladding material, propagation modes are highly confined within the waveguides, with cross-sectional dimensions on the order of a few hundred nanometers, which enables large-scale integration and compact designs. However, the small feature sizes of the waveguides raise the problem of large mode mismatches between the light source, typically the output from an optical fibre with a spot size of $\sim 10$ $\mu$m, and the sub-micron silicon waveguide with cross-sectional area of about 0.01 $\mu m^2$. Edge coupling is one solution to address this issue, and high-efficiency edge couplers with insertion losses below 0.5 dB, using lensed fiber and polished edge, has been demonstrated.[1] But this approach can only be used at the edge of the chips and the implementation of such a design requires complicated post processing, which increases the packaging cost dramatically. The alignment to such an edge coupler also requires high accuracy, which involves significant effort. Therefore, surface coupling, enabled by grating couplers, is a popular alternative. This approach addresses the mode mismatch issue and has the advantage that the coupler can be positioned anywhere on the chip. It also has the advantages of compact design, lower cost (e.g. no lensed fibers and no edge polishing), and easy-alignment. Both academic and industrial research groups have demonstrated various grating couplers with low insertion loss.[2–4] However, all of these grating couplers are achieved by "shallow etching", which requires two lithography steps. The additional lithography step increases the fabrication cost and complexity. A fully-etched grating coupler is a simpler and more economic alternative to the shallow-etched grating coupler. Fundamental building blocks of photonics circuits can be fabricated in just one step by implementing a regular fully-etched grating coupler, which offers a quick solution for prototyping. The critical issue faced by fully-etched grating coupler is the strong back reflection into the waveguide. Due to the large refractive index contrast in the grating region, the Fresnel reflection, which is the main source of back reflection, becomes much larger than that of a shallow-etched grating coupler.

Photonic crystal structures have been implemented in fully-etched grating couplers,[5] where custom silicon and buried oxide layer thickness chosen to optimize the grating coupler's performance were used, which are not available on the wafers used by most SOI foundaries. Sub-wavelength structures[6,7] have been used to improve the coupling efficiency and reduce the back reflection at the same time, but only coupling for the fundamental quasi-TM mode has been demonstrated. In addition, all of these grating couplers require adiabatic tapers on the order of hundreds of micrometers,[6] which consumes significant real-estate on the chip. In this paper, we demonstrate a fully-etched grating coupler for the fundamental quasi-TE mode, operating at 1550 nm, with reduced back reflection and improved coupling efficiency. The bandwidth of the proposed structure has been greatly improved as compared to the regular, fully-etched grating coupler. In addition, the proposed design has the potential to have a much smaller footprint.

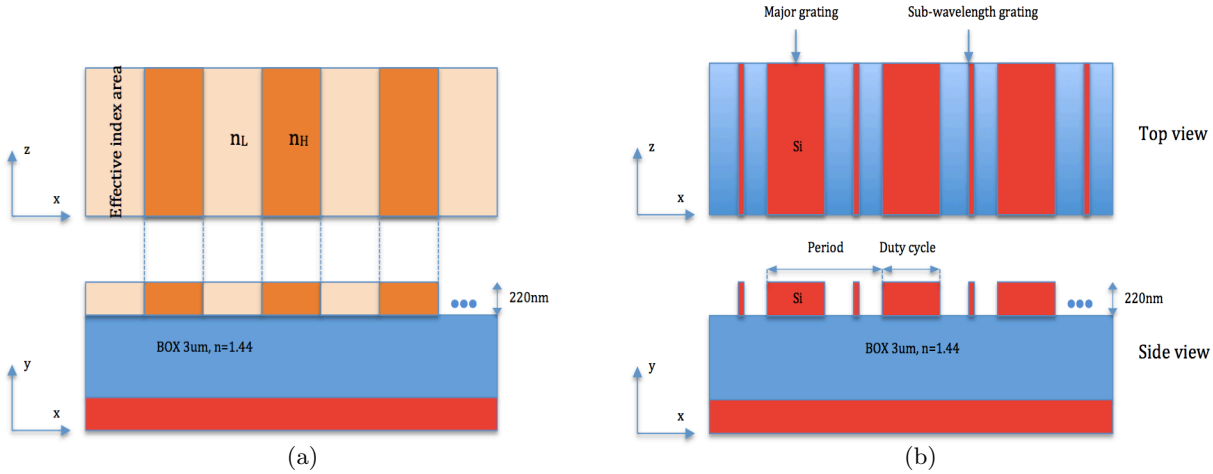


Figure 1. Schematic of the sub-wavelength, fully-etched grating coupler.

## 2. DESIGN AND SIMULATION

Our grating coupler design uses the silicon-on-insulator (SOI) wafer, with a 3 $\mu$m buried oxide and a 220 nm top silicon layer, that is used by IMEC and IME. Figure 1 is a schematic of our fully-etched grating coupler, which consists of alternating index areas (shown in Figure 1 (a)) formed by the major (wider) gratings and the minor (narrower) sub-wavelength gratings ( shown in Figure 1 (b)). The minor gratings are sufficiently small for the optical wave to see the area between the major gratings as having an average effective index. For this reason, we call our fully-etched grating coupler a sub-wavelength grating coupler in the rest of this paper.

According to effective medium theory (EMT), a zeroth-order approximation can be applied to sub-wavelength structures with period-to-wavelength ratios, defined as $R = n_{eff} \cdot \Lambda/\lambda$, much smaller than 1. Here $n_{eff}$ denotes the effective index of the quasi-TE mode in a slab waveguide with 220 nm thickness:[8]

$$\frac{1}{n_{TE}^{(0)}} = \left[\frac{ff_x}{n_c^2} + \frac{(1-ff_x)}{n_{si}^2}\right]^{1/2} \tag{1}$$

$$n_{TM}^{(0)} = \left[n_c^2 ff_x + n_{si}^2(1-ff_x)\right]^{1/2} \tag{2}$$

where $n_{TE}^{(0)}$ denotes the effective index of the quasi-TE and quasi-TM modes respectively in the effective index area, $n_c$ denotes the refractive index of the cladding material, which is air in our case ( n=1), $n_{si}$ denotes the refractive index of the sub-wavelength grating (n=3.47), and $ff_x$ is defined as the ratio of the width of the sub-wavelength grating to the width of the gap between the major gratings. Second-order EMT can be used as a more accurate approximation to explore structures with lateral feature size of the same order as the wavelength in the medium:[8]

$$n_{TE}^{(2)} = n_{TE}^{(0)}\left[1 + \frac{\pi^2}{3}R^2 {ff_x}^2(1-ff_x)^2(n_c^2-n_{si}^2)^2 \cdot (\frac{n_{TM}^{(0)}}{n_{eff}})^2(\frac{n_{TE}^{(0)}}{n_c n_{si}})^4\right]^{1/2} \tag{3}$$

Based on the above equations, we can analytically estimate the effective index of the grating. Nevertheless, numerical method are usually used to calculate the effective index of the grating.

The two-dimensional finite-difference time-domain (FDTD) method has been employed to optimize the parameters of the sub-wavelength grating coupler to achieve small insertion loss as well as small back reflection to the waveguide. A simulation model has been created within *FDTD Solutions*, a FDTD-method Maxwell equation solver from *Lumerical Solutions, Inc.* Design parameters such as the grating period, the duty cycle, the width

of the sub-wavelength grating, etc., are optimized with the built-in particle swarm algorithm.[9] The optimized sub-wavelength grating coupler has a period of 625 nm, a duty cycle of 190 nm with sub-wavelength gratings of 50 nm. The simulated insertion loss and back reflection to the waveguide of the sub-wavelength grating coupler are shown in Figure 2. The simulation results of the regular fully-etched grating coupler were also included for the purpose of comparison. The thinner lines indicate the insertion loss and back reflections of the regular fully-etched grating coupler and the thicker lines indicate those of the sub-wavelength grating coupler. Solid lines indicate the insertion losses and dash lines indicate the back reflections. As shown in Figure 2, as compared to the regular, fully-etched grating coupler, the insertion loss has been improved from -7 dB to -4 dB and the back reflection has been suppressed from -6 dB to -14 dB at 1550nm.

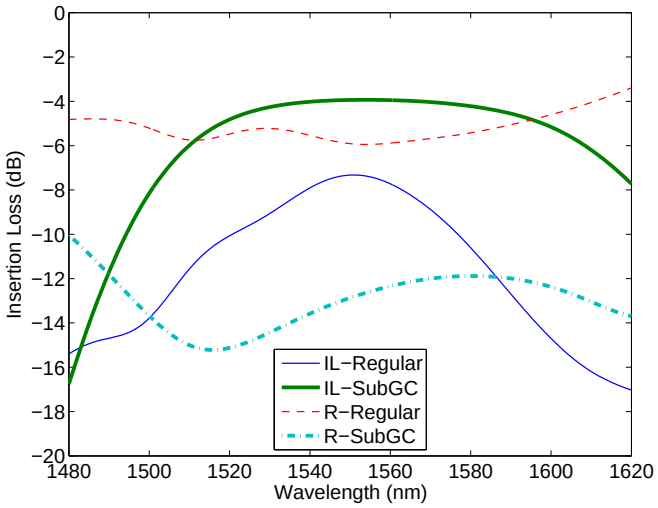


Figure 2. Simulation results of the insertion loss (IL) and back reflection to the waveguide (R) of the regular, fully-etched grating coupler and the proposed, sub-wavelength grating coupler. Thinner lines indicate the IL and R of the regular, fully-etched grating coupler and thicker lines indicate the IL and R of the sub-wavelength grating coupler. Solid lines indicate the IL and dash lines indicate the R.

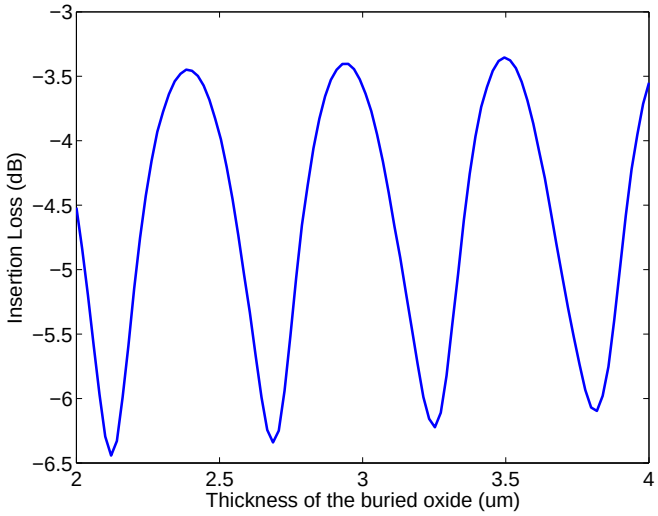


Figure 3. Insertion loss as a function of the thickness of the buried oxide.

The performance of the sub-wavelength grating coupler is optimized with the given buried oxide, i.e., 3 $\mu$m and silicon thicknesses, i.e., 220 nm. However, if a customized buried oxide were available, further improvement could be obtained by optimizing the thickness of the buried oxide. Depending on the thickness of the buried oxide, the reflected wave at the interface of the buried oxide and the silicon substrate can interfere either constructively or destructively, with the diffracted wave at the interface of the buried oxide and the grating. Figure 3 shows the insertion loss as a function of the thickness of the buried oxide. With the optimized thickness of the buried oxide, the insertion loss of the sub-wavelength grating coupler could be further improved to be -3.4 dB.

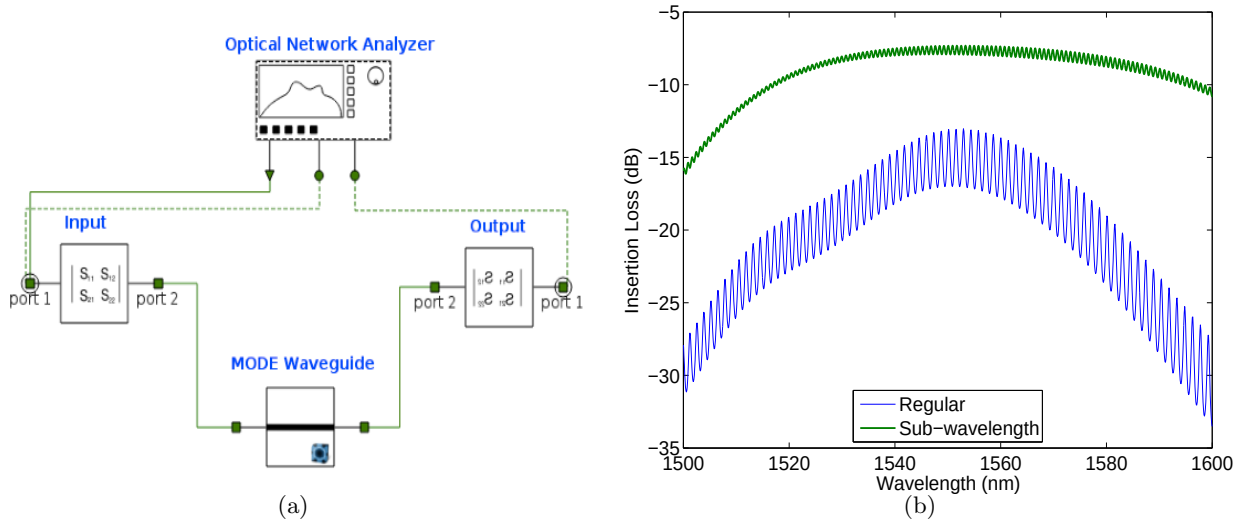


Figure 4. (a) Schematic of the input-waveguide-output circuit in *Lumerical*'s Interconnect; (b) simulation results for the input-waveguide-output circuit for the regular, fully-etched grating coupler (blue line) and the sub-wavelength grating coupler (green line). The thinner solid line is the spectral response of the regular, fully-etched grating coupler and the thicker solid line is the spectral response of the sub-wavelength grating coupler.

Figure 2 only shows the simulation results for a single grating coupler where important features such as oscillation ripples do not occur. In real photonic circuits, a pair of grating couplers are required: one input grating coupler and one output grating coupler. A Fabry-Perot cavity forms between the input and output grating couplers, where the reflected wave propagates between the two gratings and introduces ripples in the spectral responses of the photonic circuits. Simulation of a full input-waveguide-output circuit has been performed using Interconnect, a design environment for the analysis of photonic circuits from *Lumerical Solutions, Inc.* Figure 4 (a) shows a schematic of the input-waveguide-output circuit in Interconnect. A virtual optical network analyzer is employed to generate the optical signal. Grating couplers are represented by a 2-port S-parameter matrix, which is exported from FDTD solutions. The waveguide between the two grating couplers is a component which can be loaded from Mode solutions, a waveguide design environment for the planar optical waveguide from *Lumerical Solutions, Inc.* Simulation results for the input-waveguide-output circuit of the regular, fully-etched grating coupler and the sub-wavelength grating coupler are shown in Figure 4 (b). Due to the large back reflection of the regular, fully-etched grating coupler, strong ripples are seen in the spectral response of the input-waveguide-output circuit. The thinner blue line denotes the spectral response of the regular, fully-etched grating coupler and the thicker green line denotes the spectral response of the sub-wavelength grating coupler. The extinction ratio of the ripples of the regular, fully-etched grating coupler is as large as 4 dB, which has a strong impact on the performance of resonator structures such as ring resonators, Bragg gratings, and disk resonators. By implementing the sub-wavelength gratings, the index contrasts between the major gratings and the air gaps have been mitigated. Thus, the Fresnel reflections, which are the main source of back reflection of the regular fully-etched grating coupler, can be minimized. As compared with the regular, fully-etched grating coupler, the sub-wavelength grating coupler has a much weaker Fabry-Perot effect, because of the suppressed back reflection. The extinction ratio of the ripples of the sub-wavelength grating coupler is only about 0.4 dB, which is similar to

that of a shallow-etched grating coupler. The bandwidth of the sub-wavelength grating coupler is also improved, which is caused by reduced dispersion.[10] The simulated 3-dB bandwidth of the sub-wavelength grating coupler is 83.5 nm, which is much larger than that of the regular, fully-etched grating coupler.

## 3. MEASUREMENT

### 3.1 Measurement Setup

Figure 5 is an image of the automated measurement setup. The chip is placed on a platform which is on top of an angle rotator. An X-axis motorized stage and a Y-axis motorized stage are seated below the angle rotator. A fiber array ribbon is held by a custom-made aluminum fiber ribbon holder, which is suspended on top of the chip platform. An aluminum arm is used to hold the fiber ribbon holder and is attached to a second angle rotator. This second angle rotator is fixed onto a Z-axis actuator that is bolted to a raised platform so that the fiber ribbon height can be manually adjusted as needed. The ribbon-to-chip image is captured by a microscope sitting on top of the motorized stage, and is used for alignment purposes. The light source for the microscopes illuminates the chip platform at an angle from behind the fiber ribbon.

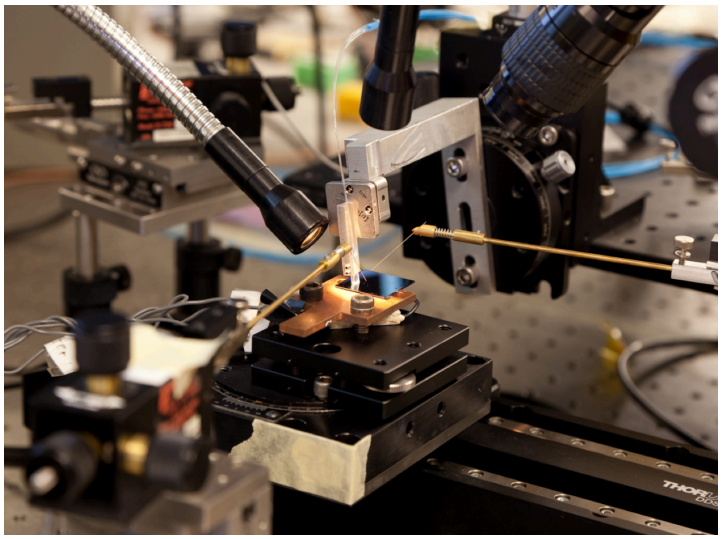

Figure 5. Automated measurement setup.

### 3.2 Measurement Results

Test structures, consisting of an input sub-wavelength grating coupler and an output sub-wavelength grating coupler, with 127 $\mu$m pitch, connected by a strip waveguide have been fabricated using electron beam lithography at the University of Washington using their JEOL JBX-6300FS E-Beam Lithography system. Regular, fully-etched grating couplers were also fabricated for comparison purposes. A comparison of the measurement and the simulation spectral responses of the sub-wavelength grating coupler is shown in Figure 6 (a). Due to the air gap between fiber array and the chip surface, there is a mismatch between the ideal condition and the real case. When we assume no air gap exists between the fiber array and the chip surface, we get the spectral response shown by the green curve, which has a lower insertion loss and broader bandwidth than the measured spectral response. When a 65 $\mu$m gap is assumed, the simulated spectral response provides a much better match to our measured spectral response. Figure 6 (b) shows the insertion loss of the input-waveguide-output circuit as a function of the gap distance between the fiber array and the chip surface. Figure 7 shows the comparison of the measurement spectra of the sub-wavelength grating coupler and the regular, fully-etched grating coupler, from which we can see that the back reflection has been reduced and the bandwidth has been improved. The measured extinction ratio of the sub-wavelength grating coupler has been suppressed from about 4 dB to 0.4 dB and the measured

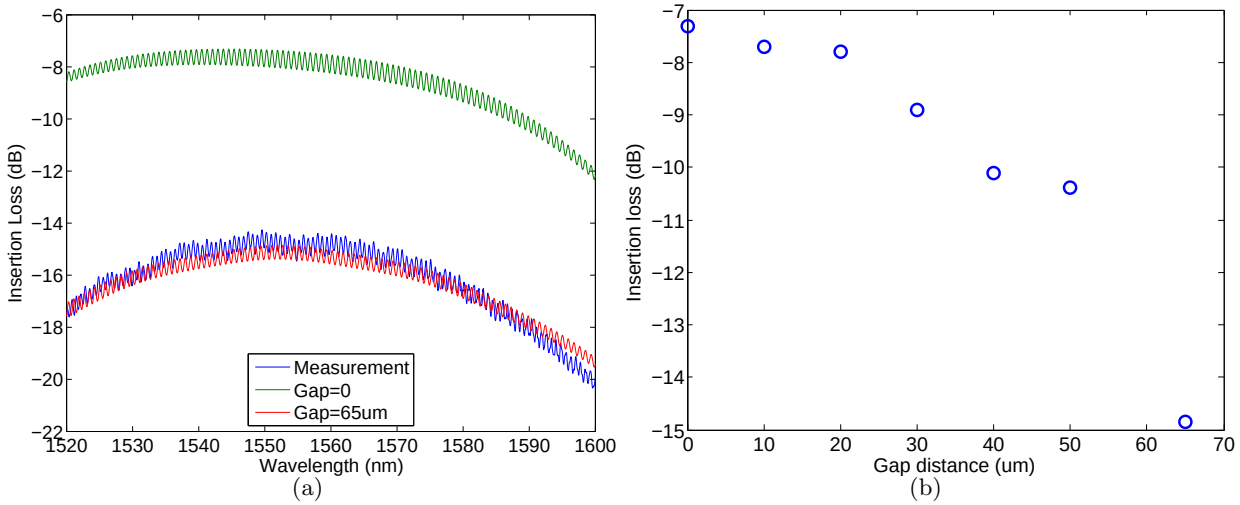


Figure 6. Spectral responses of the measured input-waveguide-output circuit (blue curve) and the simulation results for the same circuit with different air gaps between the fiber array and the chip surface; (b) Insertion loss of the input-waveguide-output circuit as a function of the gap distance between the fiber array and the chip surface.

3-dB bandwidth is 64.4 nm, which is much larger than that for the regular, fully-etched grating coupler. The insertion loss of the input-waveguide-ouput circuit is -14 dB, which also shows a little improvement.

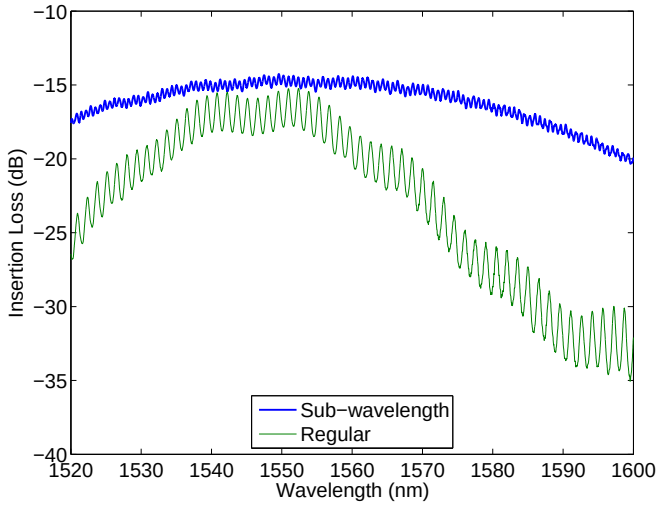


Figure 7. Measurement spectral responses for the input-waveguide-output circuit for the regular, fully-etched grating coupler (thinner green line) and for the sub-wavelength grating coupler (thicker blue line).

## 4. DISCUSSION

We have demonstrated a sub-wavelength grating coupler with straight grating lines. According to the idea demonstrated by Frederik,[11] focusing grating lines can be employed to reduce the footprint of linear gratings with long adiabatic tapers, without performance penalty. One of the advantage of our sub-wavelength grating coupler is that it is easily transformed into compact design using focusing gratings. The dimension of the sub-wavelength grating coupler is only 30 $\mu$m by 40 $\mu$m, and would be the most compact sub-wavelength grating couplers to the best of our knowledge.

## 5. CONCLUSION

In this paper, we have demonstrated a sub-wavelength, fully-etched grating coupler with reduced back reflection to the waveguide. As compared to the regular, fully-etched grating coupler, he back reflection has been suppressed by the inclusion of the sub-wavelength structures. The extinction ratio of the ripples in the spectral response has been successfully reduced from about 4 dB to 0.4 dB. The bandwidth has also been increased significantly as compared to regular, fully-etched grating couplers and a slight improvement in insertion loss has been achieved. In addition, our sub-wavelength grating coupler could be used in compact designs with focusing grating lines, which have much smaller footprints than the conventional grating couplers that use long adiabatic tapers.

## ACKNOWLEDGMENTS

We acknowledge CMC Microsystems for the provision of services that facilitated this research, and Lumerical Solutions, Inc., and Mentor Graphics for the design software. This work was supported by the Natural Sciences and Engineering Research Council of Canada, particularly under the CREATE SiEPIC program. Fabrication of the devices were conducted at the University of Washington Microfabrication/Nanotechnology User Facility, a member of the NSF National Nanotechnology Infrastructure Network. Yun Wang also acknowledges the Institute for Computing, Information, and Cognitive Systems (ICICS) at UBC for subsidizing his conference travel.

## REFERENCES

1. S. McNab, N. Moll, and Y. Vlasov, "Ultra-low loss photonic integrated circuit with membrane-type photonic crystal waveguides," *Optics Express* **11**(22), pp. 2927–2939, 2003.
2. A. Mekis, S. Gloeckner, G. Masini, A. Narasimha, T. Pinguet, S. Sahni, and P. De Dobbelaere, "A grating-coupler-enabled cmos photonics platform," *Selected Topics in Quantum Electronics, IEEE Journal of* **17**(3), pp. 597–608, 2011.
3. N. Na, H. Frish, I.-W. Hsieh, O. Harel, R. George, A. Barkai, and H. Rong, "Efficient broadband silicon-on-insulator grating coupler with low backreflection," *Optics letters* **36**(11), pp. 2101–2103, 2011.
4. G. Roelkens, D. Vermeulen, S. Selvaraja, R. Halir, W. Bogaerts, and D. Van Thourhout, "Grating-based optical fiber interfaces for silicon-on-insulator photonic integrated circuits," *Selected Topics in Quantum Electronics, IEEE Journal of* **17**(3), pp. 571–580, 2011.
5. L. Liu, M. Pu, K. Yvind, and J. M. Hvam, "High-efficiency, large-bandwidth silicon-on-insulator grating coupler based on a fully-etched photonic crystal structure," *Applied physics letters* **96**(5), pp. 051126–051126, 2010.
6. R. Halir, P. Cheben, S. Janz, D.-X. Xu, Í. Molina-Fernández, and J. G. Wangüemert-Pérez, "Waveguide grating coupler with subwavelength microstructures," *Optics letters* **34**(9), pp. 1408–1410, 2009.
7. R. Halir, P. Cheben, J. Schmid, R. Ma, D. Bedard, S. Janz, D.-X. Xu, A. Densmore, J. Lapointe, and I. Molina-Fernández, "Continuously apodized fiber-to-chip surface grating coupler with refractive index engineered subwavelength structure," *Optics letters* **35**(19), pp. 3243–3245, 2010.
8. X. Chen and H. K. Tsang, "Polarization-independent grating couplers for silicon-on-insulator nanophotonic waveguides," *Optics Letters* **36**(6), pp. 796–798, 2011.
9. J. Robinson and Y. Rahmat-Samii, "Particle swarm optimization in electromagnetics," *Antennas and Propagation, IEEE Transactions on* **52**(2), pp. 397–407, 2004.
10. X. Chen, K. Xu, Z. Cheng, C. K. Fung, and H. K. Tsang, "Wideband subwavelength gratings for coupling between silicon-on-insulator waveguides and optical fibers," *Optics Letters* **37**(17), pp. 3483–3485, 2012.
11. F. Van Laere, T. Claes, J. Schrauwen, S. Scheerlinck, W. Bogaerts, D. Taillaert, L. O'Faolain, D. Van Thourhout, and R. Baets, "Compact focusing grating couplers for silicon-on-insulator integrated circuits," *Photonics Technology Letters, IEEE* **19**(23), pp. 1919–1921, 2007.